Flattening and Solidification of Thermally Sprayed Particles

C. Moreau, P. Cielo, and M. Lamontagne

In this article, molybdenum particles were plasma sprayed on copper, zirconia, and glass substrates. The impact of the molten particles was monitored using a fast two-color optical fiber pyrometer focused on a small spot on the substrate surface. The apparent duration of the flattening process and the cooling speed, both determined from the pyrometer signals, were found to depend on the substrate conditions and to vary with coating thickness. The substrate material and its roughness were also found to influence the texture in the sprayed coatings. Furthermore, a transient thermal flow numerical model was used to compute reliable thermal histories of the impinging particles and the underlying lamellae, the interfacial thermal resistance being determined by comparison of experimental thermograms with computed ones.

1. Introduction

In a previous study,[1] the cooling rate of plasma sprayed molybdenum particles impinging on different substrate materials was found to increase as a function of coating thickness. This increase was attributed to lower thermal resistance at the lamella/lamella interface than at the lamella/substrate interface for all considered materials (i.e., copper, zirconia, and glass) and to the low thermal conductivity of the zirconia and glass substrates. Moreover, the lamella microstructure was found to vary through the coating thickness. Within the coating, the lamellae had a columnar structure, whereas at the substrate interface, this structure was absent. This microstructural change was related to the superior wettability, by the molten molybdenum particles, of the already deposited molybdenum lamellae compared to the wettability of the other substrate materials. The substrate nature was found to influence not only the lamella microstructure, but also the lamella morphology.

In the present work, other aspects related to the impact of the molten molybdenum particles were investigated. Using the results presented in Ref 1, the thermal history of the impinging particles, as well as the thermal histories of the already deposited lamellae and of the substrate surface, are computed. Such computation permits investigation of the subsequent heat treatment of lamellae due to the impact of overlapping particles. Moreover, the apparent flattening time of the particles impinging on different substrate surfaces and its evolution with the coating thicknesses are experimentally determined. Such an investigation may be useful to compare with predictions of theoretical models such as those of Madejski[2,3] and Fedorchenko *et al.*[4] Finally, the coating surface texture is investigated using X-ray diffraction to characterize the solidification process.

Key Words: lamellar temperature, molybdenum particles, numerical model, temperature diagnostics, transient thermal flow

C. Moreau, P. Cielo, and **M. Lamontagne,** National Research Council Canada, Industrial Materials Institute, Boucherville, Québec, Canada.

2. Experimental Procedure

Details of the experimental setup have been published elsewhere,[1,5] and only a brief description will be given here. As shown in Fig. 1, particles were sprayed through a 2-mm hole drilled in a metal mask and impinged on the substrate located about 12 cm from the torch. The thermal radiation emitted by a hot particle hitting the substrate in the field of view of the pyrometer head (located at the bottom of Fig. 1) was collected and transmitted through the optical fiber to a detection cabinet containing two photodetectors (D_1 and D_2) filtered at 900 and 700 nm, respectively. The time response of the two photodetectors and the following recording electronics was less than 0.1 μs. The particle surface temperature was computed, after calibration,

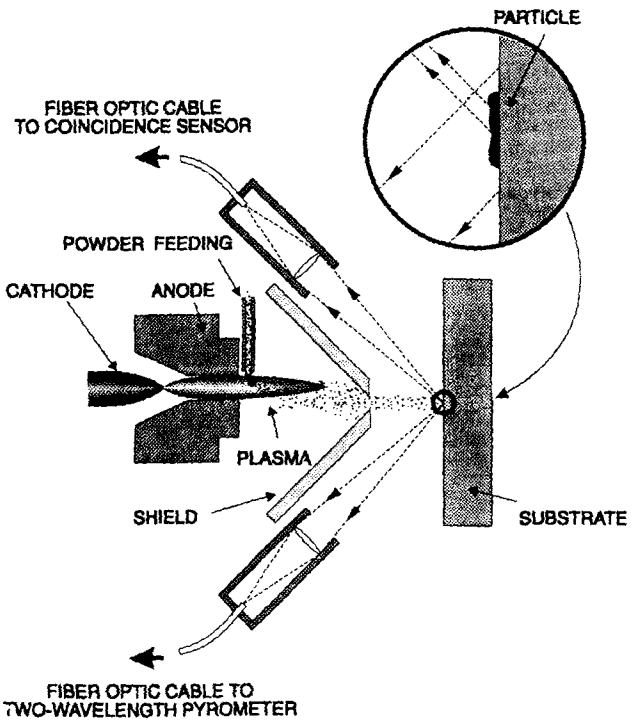

Figure 1 Schematic of the experimental setup.

from the ratio of the two photodetector outputs. The diameter of the pyrometer-monitored area was about 400 μm.

A second detection head (located at the top of Fig. 1) was used to discriminate against in-flight particles intersecting the pyrometer field of view, but impinging on the substrate outside the monitored area. The second head was focused on the center of the pyrometer-monitored area, and the collected radiation was transmitted using a second optical fiber to a third photodetector located in the detection cabinet. A simultaneous detection of a particle by both heads ensured that the event corresponded to a particle impinging on the substrate surface in the pyrometer-monitored area.

Plasma spraying was carried out with a Plasmadyne SG100 gun operating at 600 A and 37 V. The arc gas consisted of a mixture of 50 l/min argon and 25 l/min helium. The molybdenum powders (Amperit 102.90, –45 +22 μm) were injected radially at the exit of the plasma gun at a low feeding rate ranging from 3 to 14 g/min. Such low feeding rates were used to avoid simultaneously detecting radiation from more than one particle by the pyrometer head and to prevent the 2-mm hole in the metal mask from clogging. When a splat event was detected after a gun traverse in front of the hole in the metal mask, the recorded signals were transferred to a microcomputer and saved on a hard disk, and the number of gun passages was noted. The procedure was then repeated to record new events. The actual coating thickness was estimated after spraying by metallographic inspection of the coating cross section. Molybdenum coatings were sprayed on copper, glass, and zirconia substrates after grit blasting with a fine grit to promote particle adhesion on the substrate without favoring particle disintegration.

Surface roughness (arithmetical average) was determined using Surtronic 3 profilometer. X-ray diffraction patterns were obtained with the Cu K_α line using a Philips PW1840 diffractometer. Texture measurements were carried out by computing the intensity ratio of the (200) and (110) diffraction peaks.

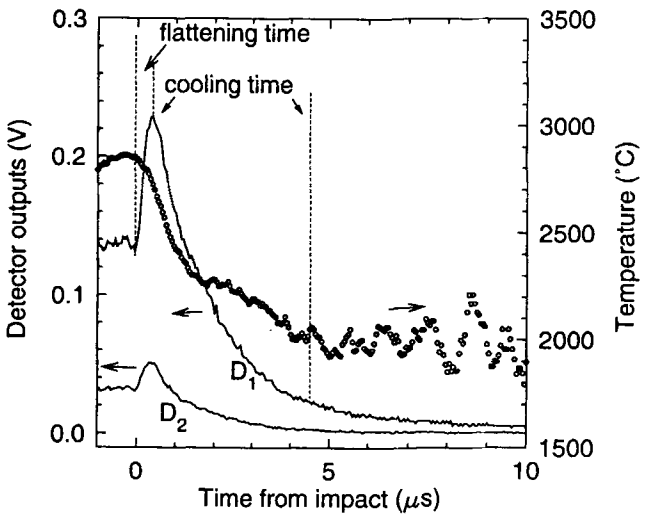

Figure 2 Example of collected signals and the corresponding temperature curve for a particle impact. The apparent flattening time and cooling time are computed using signal D_1 as indicated in the figure.

3. Results and Discussion

Figure 2 is an example of a splat event recorded when a molybdenum particle impinges on the surface of a 60-μm-thick coating already deposited on a glass substrate. Signals D_1 and D_2 correspond to the light intensity collected by the two detectors of the pyrometer filtered at 900 and 700 nm, respectively. The surface temperature evolution of the impinging particle obtained from the ratio of the detector outputs D_1 and D_2 is also shown in Fig. 2. At the moment of impact, the area of the sprayed particle increases rapidly, producing a sudden increase in the detected radiation, as observed in both detector outputs shown in Fig. 2. Light collected before particle impact comes from the in-flight particle and thus permits computation of the particle temperature immediately prior to impact. After the initial contact, the particle area continues to increase, while its temperature begins to decrease, leading to a maximum in the signal intensity. Afterwards, when the flattened particle has reached its final diameter, the radiation intensity decreases as the particle cools.

3.1 *Evolution of Flattening and Cooling Times*

The flattening time of a particle impinging on a hard surface can be defined as the time required for the particle to deform and spread until its maximum area is reached. In this article, the apparent flattening time was determined by measuring the time lapse between the rapid signal increase at 900 nm corresponding to the particle contact with the substrate and the occurrence of the maximum signal intensity. This time is termed "apparent" because it may be different from the real flattening time if the temperature drop occurring during the flattening process is large enough so that the light intensity emitted by the spreading particle reaches a maximum before flattening is completed. The cooling time is estimated by measuring the time required for the 900-nm signal to decrease by one order of magnitude from its maximum value. This corresponds to a temperature drop of about 800 to 900 °C.[1]

The dependence of the apparent flattening time on the coating thickness is shown in Fig. 3(a), (b), and (c) for coatings deposited on zirconia, glass, and copper, respectively. The corresponding cooling times from Ref 1 are also shown in Fig. 3(d) to 3(f). As discussed in the Introduction, the cooling time is shorter for a thicker coating, and this is related to the higher interfacial thermal resistance at the molybdenum/substrate interface than at the molybdenum/molybdenum interface and to the lower thermal conductivity of zirconia and glass compared to that of molybdenum. A corresponding decrease is observed for the apparent flattening time. Indeed, it varies from about 1.8 μs at the zirconia and the glass interfaces to about 0.8 μs over a built-up coating. The flattening time is slightly lower on the copper substrate.

Figure 4 shows the evolution of the computed light intensity emitted by a particle experiencing different cooling rates after impact, assuming that the particle diameter increases linearly with time from 40 μm at the impact moment to a final diameter of 80 μm after 1.8 μs. These values correspond to those observed experimentally. The assumed linear diameter increase with time compares well with the theoretical results of Madejski.[2,3] Figure 4 shows that the maximum signal intensity, as indicated by the dashed line, corresponds to the end of the flattening process,

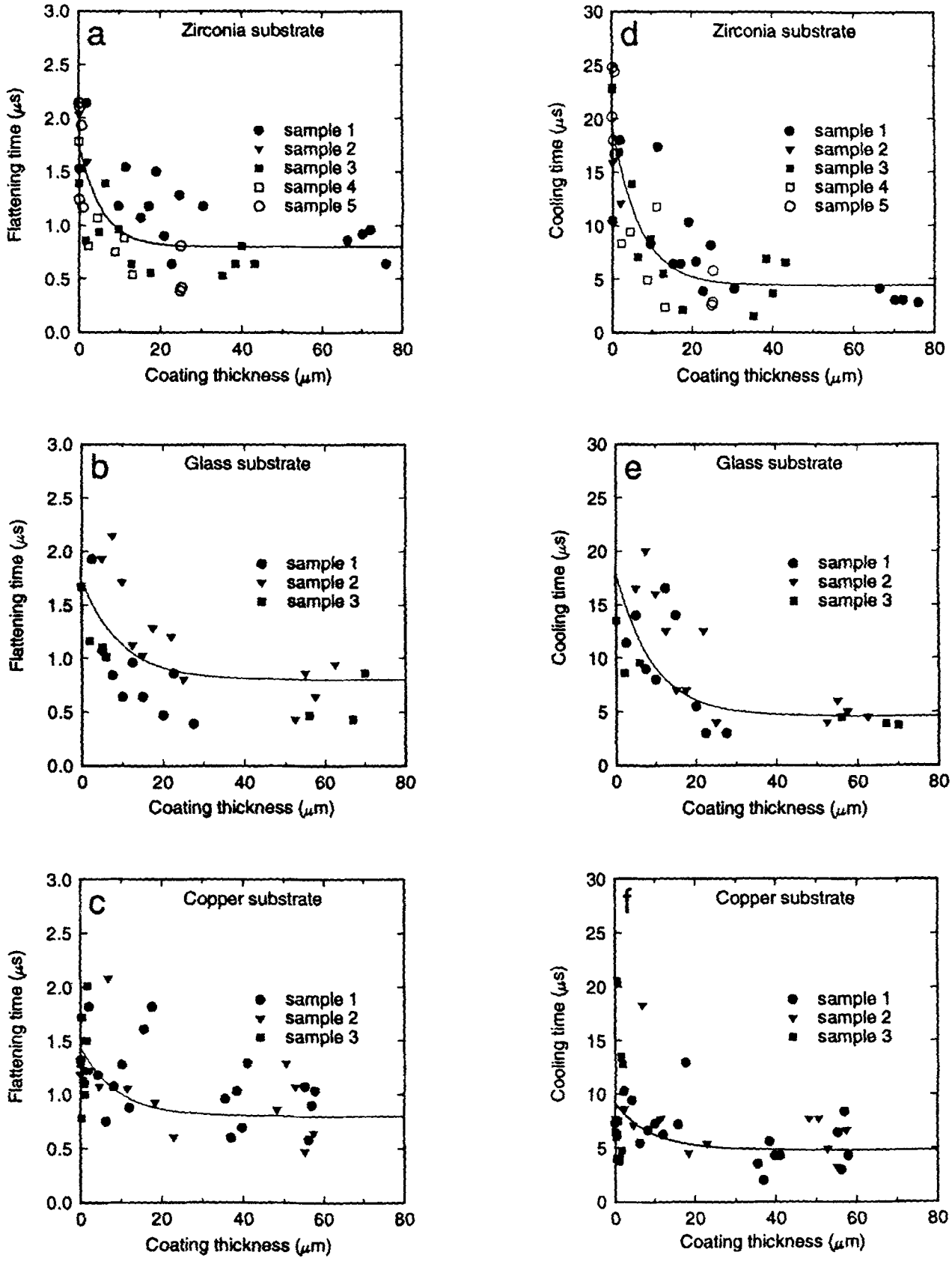

Figure 3 Apparent flattening time and cooling time as a function of coating thickness on zirconia (a and d), glass (b and e), and copper (c and f) substrates. Each point corresponds to an individual particle impact.

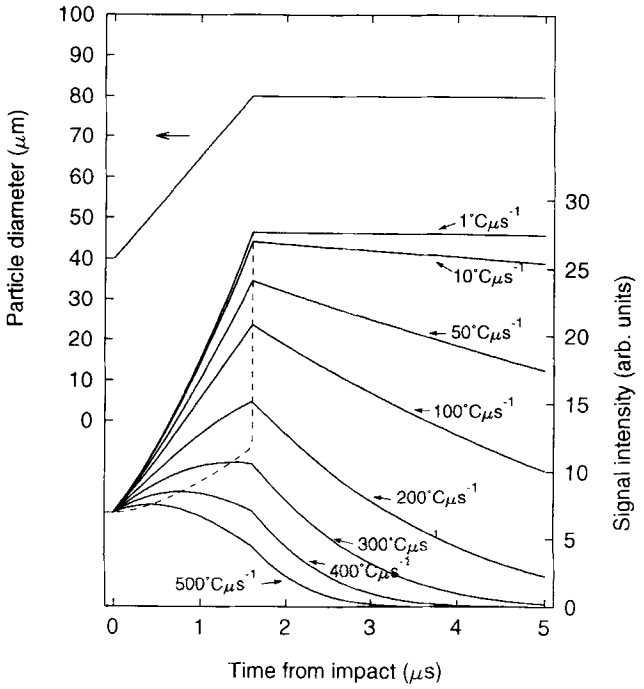

Figure 4 Evolution of particle diameter and light signal intensity emitted by a spreading particle as computed assuming different cooling rates after impact.

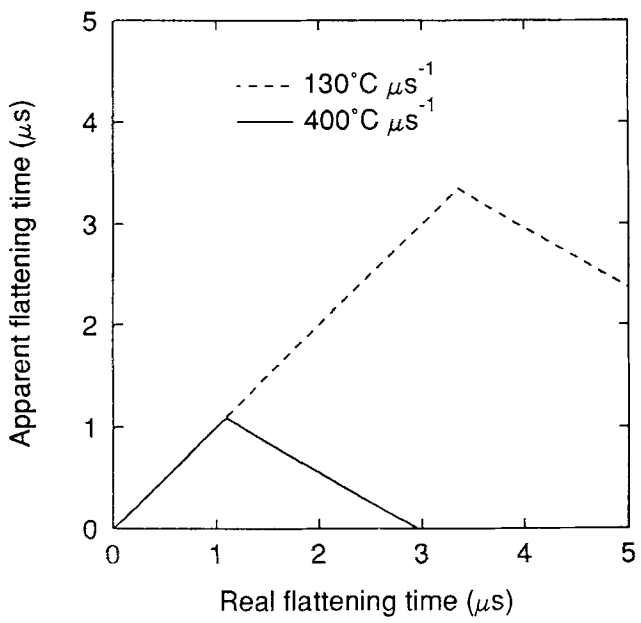

Figure 5 Relation between the apparent and the real flattening times for cooling rates before solidification of 130 and 400 °C/μs.

if the cooling rate after impact is lower than about 250 °C/μs. For higher cooling rates, the decrease of the light intensity due to the temperature drop during the flattening process compensates for the signal increase due to the increase in emitting area of the particle during spreading. The maximum signal intensity is thus reached before the end of the flattening process, leading to a decrease in the apparent flattening time.

As shown in Fig. 3, when a molybdenum particle impacts the zirconia or the glass substrate, its cooling time is about 18 μs and corresponds to a cooling rate of 40 to 50 °C/μs. However, the cooling rate is more rapid before the solidification plateau, being about 130 °C/μs (see below, Fig. 6). Figure 5 shows the expected relationship between the apparent and the real flattening times, assuming that a cooling speed of 130 °C/μs prevails during the flattening process. In the present case, the apparent flattening time is equal to the real flattening time for times shorter than 3.2 μs. For longer flattening times, the apparent flattening time decreases due to the surface temperature drop during the flattening process. According to Fig. 3(a) and (b), the apparent flattening time of particles impinging on the zirconia and glass substrates is about 1.8 μs. Thus, it is likely that this time is a real indication of the flattening process duration. It is interesting to note that the corresponding mean flattening speed is about 10 ms^{-1} because the particle radius increases from about 20 to 40 μm during this time. This speed is one order of magnitude lower than the expected velocity of the in-flight particles immediately before the impact.[6,7]

When molybdenum particles impinge on the surface of the already deposited molybdenum coating, the cooling rate before solidification increases to nearly 400 °C/μs, and the apparent flattening time decreases to 0.8 μs. In this case, as shown in Fig. 5, the real flattening time, which may range from 0.8 to about 1.6 μs, cannot be determined for certain. Consequently, it is not possible to conclude that the apparent flattening time change with the coating thickness observed in Fig. 3 corresponds to a real flattening time decrease. The flattening time might depend on the nature of the surface on which the particles impinge. Indeed, the wettability and roughness of the underlying surface may influence the flow conditions within the molten droplets during spreading.

3.2 *Computed Thermal Histories of Sprayed Lamellae*

The thermal histories of the first and second particles after impingement on glass and copper substrates are illustrated in Fig. 6. These curves were computed using the transient thermal flow numerical model described in Ref 1. In the present case, the lamellae were represented by a disk composed of four series of toroidal elements to obtain a better representation of the temperature gradient through the lamella thickness. Uniform thermal resistances of 0.3×10^{-6} and 0.9×10^{-6} $m^2 \cdot kW^{-1}$ were assumed at the molybdenum/molybdenum interface and at the molybdenum/substrate interface, respectively. These values were obtained by comparison of experimental thermograms with computed ones, so they adequately represent the actual interfacial thermal properties. When the first particle lies on the glass surface, it cools down relatively slowly due to the interfacial thermal resistance and to the low glass thermal conductivity, leading to substantial heating of the glass surface up to 1350 °C after 15 μs. On the other hand, when the particle impinges on copper, the heat dissipates rapidly through the substrate, and the substrate surface temperature does not exceed 170 °C. When a second particle impinges on the top of the first solidified lamella, this first lamella is reheated, and its thermal history depends on the substrate material, as shown in Fig. 6(b) and (d) for the glass

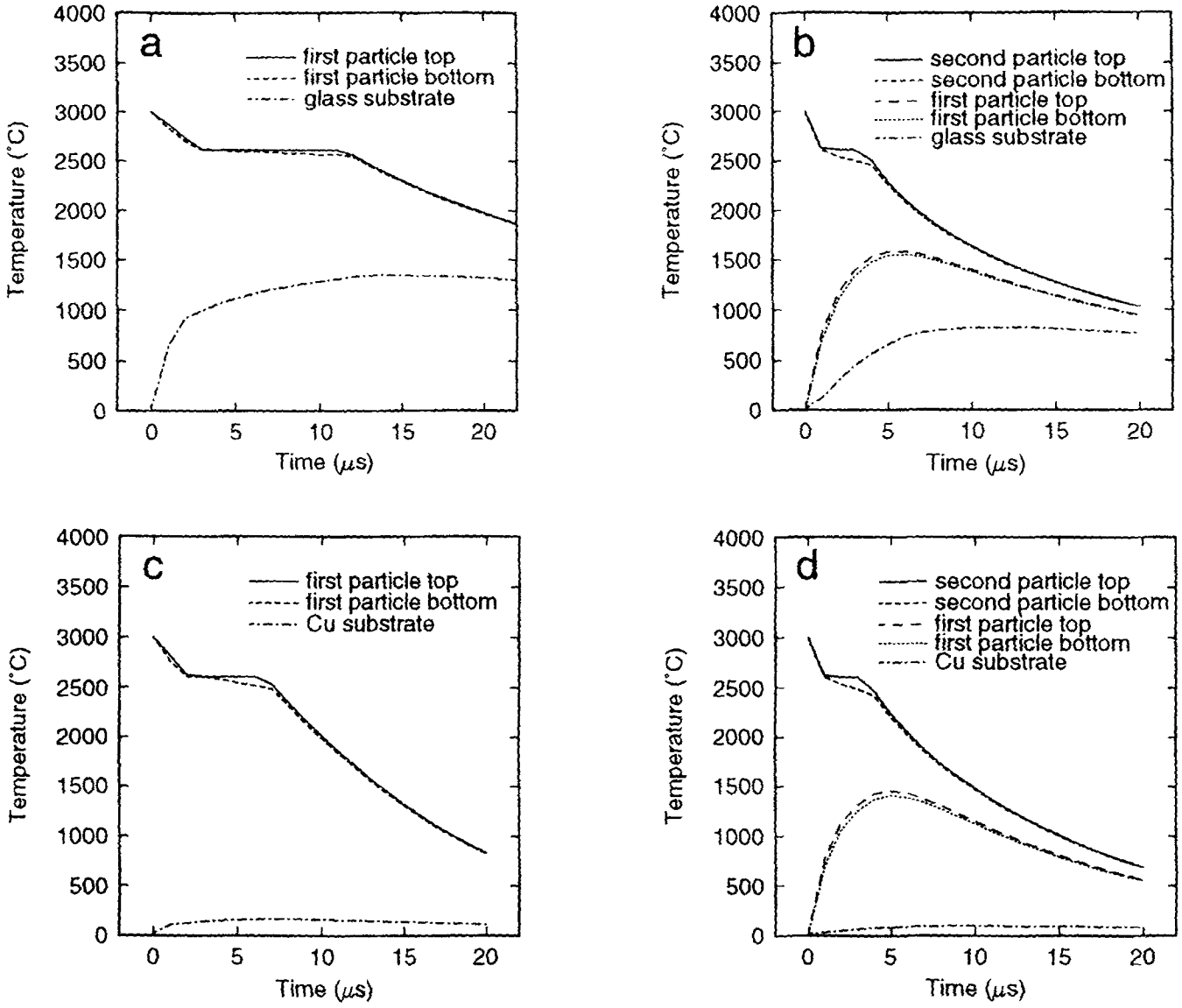

Figure 6 Computed temperature evolution after impingement of the first and the second particles on glass (a and b) and copper (c and d) substrates.

and copper substrates, respectively. In both cases, the cooling time of the impinging particle is substantially reduced compared to the first one and is nearly equal to the cooling rate obtained when particles impinge on a thick coating. The underlying lamella is reheated to about 1600 °C on the glass substrate (Fig. 6b), whereas it reaches only about 1450 °C when the coating is deposited on copper (Fig. 6d). Such a relatively high temperature is expected to promote adhesion between lamellae, leading to good cohesion of the sprayed coating.

When many particles have already been deposited, the thermal properties of the substrate material are no longer important. In this case, the thermal histories of an impinging particle and of the lamella immediately under it are very similar to those illustrated in Fig. 6(d). However, the maximum temperature of the underlying lamella is reduced to 1250 °C due to the lower interfacial thermal resistance.

3.3 *Texture Measurements*

As discussed above, the thermal histories of the first particle impinging on the bare substrate surface and of subsequent particles impinging on already deposited lamellae are different; the cooling rate and the solidification rate are lower at the substrate surface. Information about the solidification process may be obtained by texture measurements. Indeed, in conditions of rapid solidification encountered in plasma spraying, the solidification front progresses rapidly within the lamellae, favoring the fastest crystal growth direction. Table 1 gives the texture measurement results performed on the front and substrate sides of molybdenum coatings sprayed on glass and copper substrates. Molybdenum has a body-centered cubic structure, and such a metal always has its columnar grains with ⟨200⟩ parallel to the direction of heat flow.[8] Results in Table 1 indicate a strong ⟨200⟩ pre-

Table 1 Texture Measurement I(200)/I(110) on Plasma-Sprayed Molybdenum Coating Surfaces I(200)/I(110) = 0.20 for the Starting Powder

Substrate	Grit blasted		Polished
	Front side	Substrate side	Substrate side
Glass	0.30	0.24	0.22
Copper	0.35	0.22	0.30

ferred crystal orientation on the coating front side, indicating that heat flux and crystal growth progressed perpendicularly to the surface. On the grit-blasted substrate side, no such textures are evident. In an earlier study, Sampath and Herman reported a texture difference between the front and the back sides of nickel and nickel-aluminum sprayed coatings.[9] They attributed this difference to the change of orientation of ⟨200⟩ textured lamellae relative to the substrate normal due to the surface roughness. The measured textures were maximum when parallel lamellae solidified on a polished substrate surface and minimum on the front side where lamellae were randomly oriented due to the roughness of the coating surface. The surface roughness of the molybdenum sprayed coatings on the front and on the substrate sides was measured and results are given in Table 2. In the present case, a surface roughness effect like the one described by Sampath and Herman cannot be the only factor responsible for the noted texture difference, because the substrate side of the coating sprayed on the polished glass substrate has no evident ⟨200⟩ texture, whereas its front side presents such a strong texture.

This absence of preferred orientation observed on the substrate side may occur if solidification does not proceed in a direction perpendicular to the substrate surface, but proceeds in multiple directions. This is consistent with the absence of a columnar structure perpendicular to the substrate surface noted in lamellae at the coating/substrate interface.[1] Multiple direction growth may develop if nucleation occurs uniformly within the lamellae, leading to an equiaxed structure, or if heat is removed from the lamella through few real contact points at the coating/substrate interface, leading to growth of randomly oriented elongated grains. This situation may occur if air is entrapped between the molten impinging particles and the substrate surface, leading to a reduced real contact area between them.[10-12]

The coating front side exhibits the highest roughness, but also presents many relatively flat regions formed by the last deposited lamella. The zones between these regions are very rough leading to a high global surface roughness, as indicated in Table 2. On the other hand, the surface of the grit-blasted substrates has a fine uniformly distributed roughness that is replicated on the substrate side of the sprayed coatings. This fine roughness may be responsible for the lower ⟨200⟩ texture noted on the substrate side compared to that on the front side.

A significant texture is observed when molybdenum is sprayed on a polished copper substrate, but not on a polished glass substrate, as shown in Table 1. The absence of texture noted on the polished glass substrate may be related to the low glass thermal conductivity that reduces the lamella cooling rate and to the different wetting behavior of the molten molybdenum metal on this material. These results show that the flattening and solidification processes are strongly influenced by the underlying surface conditions.

Table 2 Surface Roughness (R_a) of Grit-Blasted Substrates and Coatings

Substrate	Substrate roughness (R_a), μm	Coating roughness (R_a), μm	
		Substrate side	Front side
Glass	1.8 ± 0.2	1.9 ± 0.1	5.0 ± 0.3
Copper	1.0 ± 0.1	0.9 ± 0.1	5.5 ± 0.6

Note: The error corresponds to one standard deviation.

4. Conclusion

Flattening and solidification of thermal sprayed particles impinging on a substrate surface are very complex phenomena. They involve very rapid changes in the dynamic and thermal state of the molten particles that depend on many factors, some of which are unknown or not well known. In this article, these processes were experimentally investigated using a fast two-color pyrometer focused on the substrate surface and X-ray diffraction for texture measurements on the coating surfaces. From the pyrometer signals, the apparent flattening time and the cooling time of the impinging droplets were found to depend on the substrate material and to decrease with the coating thickness. The decrease of the apparent flattening time with the coating thickness was likely due to the higher cooling rate of the molten droplets when they impinge on already deposited molybdenum lamellae. On the other hand, when the cooling rates were relatively low (glass or zirconia substrates), the apparent flattening time was found to correctly represent the real flattening time. The thermal histories of the impinging particles and the underlying lamellae, computed using experimentally determined interfacial thermal resistances, showed that the first and the second particle histories are influenced by the substrate conditions. Moreover, the roughness and the nature of the surface on which the molten particles impinge were found to have a significant effect on the sprayed coating texture, revealing a modification of the solidification process.

Acknowledgments

The authors wish to acknowledge Sylvain Bélanger for its technical assistance and Patrick Gougeon, Richard Neiser, and Sanjey Sampath for fruitful discussions during the manuscript preparation. This work is based on a presentation made at the 13th International Conference on Thermal Spraying, Orlando, FL, USA, 1992.

References

1. C. Moreau, M. Lamontagne, and P. Cielo, Influence of the Coating Thickness on the Cooling Rate of Plasma-Sprayed Particles Impinging on a Substrate, *Surf. Coat. Technol.*, Vol 53, 1992, p 107-114; and *Thermal Spray Coatings: Properties, Processes and Applications*, T.F. Bernecki, Ed., ASM International, 1992, p 237-243.
2. J. Madejski, Solidification of Droplets on a Cold Substrate, *Int. J. Heat Mass Transfer*, Vol 19, 1976, p 1009-1013.

3. J. Madejski, Droplets on Impact with a Solid Surface, *Int. J. Heat Mass Transfer*, Vol 26 (No. 7), 1983, p 1095-1098.
4. A.I. Fedorchenko and O.P. Solonenko, Dynamics of Crystallization Processes of Molten Particles at Their Interaction with Surface, *Plasma Jets*, O.P. Solonenko and A.I. Fedorchenko, Ed., VSP, 1990, p 283-297.
5. C. Moreau, P. Cielo, M. Lamontagne, S. Dallaire, and M. Vardelle, Impacting Particle Temperature Monitoring During Plasma Spray Deposition, *Meas. Sci. Technol.*, Vol 1, 1990, p 807-814.
6. M. Vardelle, A. Vardelle, P. Fauchais, and M.I. Boulos, Plasma-Particle Momentum and Heat Transfer: Modelling and Measurements, *AIChE J.*, Vol 29 (No. 2), 1983, p 236-243.
7. J.R. Fincke and W.D. Swank, Simultaneous Measurement of Ni-Al Particle Size, Velocity, and Temperature in Atmospheric Thermal Plasmas, *Thermal Spray Research and Applications*, T.F. Bernecki, Ed., ASM International, 1991, p 39-43.
8. C.S. Barrett and T.B. Massalski, *Structure of Metals*, 3rd ed., Pergamon Press, 1980, p 536.
9. S. Sampath and H. Herman, Microstructural Development of Plasma Sprayed Coatings, *Proc. 12th Int. Conf. Thermal Spraying*, I.A. Bucklow, Ed., The Welding Institute, London, 1989, p 53-1 to 53-10.
10. R. McPherson, A Model for the Thermal Conductivity of Plasma-Sprayed Ceramic Coatings, *Thin Solid Films*, Vol 112, 1984, p 89-95.
11. R. McPherson, A Review of Microstructure and Properties of Plasma Sprayed Ceramic Coatings, *Surf. Coat. Technol.*, Vol 39/40, 1989, p 173-181.
12. R. McPherson, The Relationship between the Mechanism of Formation, Microstructure and Properties of Plasma-Sprayed Coatings, *Thin Solid Films*, Vol 83, 1981, p 297-310.